JACS
JOURNAL OF THE AMERICAN CHEMICAL SOCIETY

Article

pubs.acs.org/JACS

Human Telomere Sequence DNA in Water-Free and High-Viscosity Solvents: G-Quadruplex Folding Governed by Kramers Rate Theory

Ford M. Lannan, Irena Mamajanov, and Nicholas V. Hud*

School of Chemistry and Biochemistry, Petit Institute for Bioengineering and Bioscience, Georgia Institute of Technology, Atlanta, Georgia 30332, United States

Supporting Information

ABSTRACT: Structures formed by human telomere sequence (HTS) DNA are of interest due to the implication of telomeres in the aging process and cancer. We present studies of HTS DNA folding in an anhydrous, high viscosity deep eutectic solvent (DES) comprised of choline choride and urea. In this solvent, the HTS DNA forms a G-quadruplex with the parallel-stranded ("propeller") fold, consistent with observations that reduced water activity favors the parallel fold, whereas alternative folds are favored at high water activity. Surprisingly, adoption of the parallel structure by HTS DNA in the DES, after thermal denaturation and quick cooling to room temperature, requires several months, as opposed to less than 2 min in an aqueous solution. This extended folding time in the DES is, in part, due to HTS DNA becoming kinetically trapped in a folded state that is apparently not accessed in lower viscosity solvents. A comparison of times required for the G-quadruplex to convert from its aqueous-preferred folded state to its parallel fold also reveals a dependence on solvent viscosity that is consistent with Kramers rate theory, which predicts that diffusion-controlled transitions will slow proportionally with solvent friction. These results provide an enhanced view of a G-quadruplex folding funnel and highlight the necessity to consider solvent viscosity in studies of G-quadruplex formation in vitro and in vivo. Additionally, the solvents and analyses presented here should prove valuable for understanding the folding of many other nucleic acids and potentially have applications in DNA-based nanotechnology where time-dependent structures are desired.

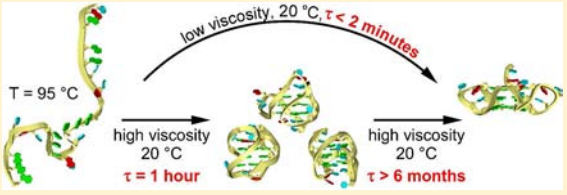

INTRODUCTION

The ends of eukaryotic chromosomes are protected from degradation and fusion by telomeres, DNA−protein complexes that are maintained by telomerase.[1,2] Telomere DNA is comprised of short repeats, for example, $d(TTAGGG)_n$ in humans, with a duplex region and an extended 3′-overhang of the G-rich strand.[3,4] DNA sequences derived from the telomeres of various species, including the human telomere sequence (HTS), form G-quadruplex structures in vitro.[5] It has been proposed that stabilizing telomere G-quadruplex structures in vivo is a possible means of cancer therapy, as G-quadruplex formation could inhibit telomerase, which may, in turn, promote apoptosis in rapidly proliferating cancer cells.[6,7]

The design and screening of ligands that target the 3′-overhang of telomere DNA is complicated by the fact that HTS-derived DNA sequences are highly polymorphic in vitro; at least five distinct folds have been experimentally verified, and even more are possible.[8−10] The actual structure of the G-rich single-stranded overhang of human telomere DNA in vivo is the subject of a debate that is fueled by reports that HTS DNA forms antiparallel-stranded G-quadruplexes in aqueous solution, but a parallel-stranded structure in the crystal state.[11] Recent investigations have explored the influence of molecular crowding[12,13] and reduced water activity[14−16] on the equilibrium-favored HTS structure, motivated by the hypothesis that the cellular milieu (and crystallization conditions) could dictate G-quadruplex structure. These studies have demonstrated the ability of cosolvents to radically alter the structure of G-quadruplexes formed by HTS DNA sequences, but questions still remain regarding the origins of structure selection (e.g., the relative contributions of crowding versus dehydration), and regarding which fold is of most physiological relevance.[17−20]

For two decades, studies of protein folding in solutions containing viscogens have provided valuable information, such as the relative importance of entropic versus enthaplic barriers to a folding pathway.[21−28] In contrast, the potential usefulness of altering viscosity to study nucleic acid folding has been virtually unexplored, with the only two published studies focused on DNA hairpin formation.[29,30] Here, we present investigations of G-quadruplex formation by HTS-derived DNA in a solvent with extremely low water content and high viscosity. These studies were enabled by our recent discovery that DNA and RNA secondary structures are stable in two anhydrous solvents, that is, an ionic liquid and a deep eutectic solvent (DES).[31] The DES solvent is composed of one part choline chloride and two parts urea.[32] We now demonstrate that viscous choline chloride−urea (ChCl−urea) solvents, with and without added water, greatly alter the folding of HTS DNA. Application of Kramers rate theory[33−35] to the observed kinetics of G-quadruplex folding/refolding provides insights

Received: April 11, 2012
Published: June 1, 2012

   dx.doi.org/10.1021/ja303499m | J. Am. Chem. Soc. 2012, 134, 15324−15330

into the folding pathway, such as identification of diffusion-controlled steps. These results demonstrate the need to consider viscosity effects on thermodynamic parameters obtained from G-quadruplex folding studies in solvents that contain crowding and dehydrating agents. Our results also demonstrate that solvent viscosity can be used to tune the kinetics of unimolecular G-quadruplex folding on time scales that range from minutes to months at room temperature. A similar phenomenon is likely to be associated with other DNA and RNA structures in high viscosity solvents.

RESULTS

Human Telomere Sequence DNA Adopts a Parallel-Stranded Fold in a Water-Free DES. Determining the folded structure of a nucleic acid in the water-free choline chloride–urea (ChCl–urea) DES presented an experimental challenge due to the high viscosity of this solvent (ca. 1000 cP at 20 °C),[32] as high viscosity precludes structure determination by NMR spectroscopy. Circular dichroism (CD) spectroscopy is compatible with the ChCl–urea DES and can be used to distinguish between different classes of G-quadruplex folds.[36−38] However, de novo G-quadruplex structure determination by CD is not possible.[38] Fortunately, Heddi and Phan have recently provided CD spectra for the HTS-derived oligonucleotide d[$TAG_3(TTAG_3)_3$] (*Htelo1*) for solution conditions in which its G-quadruplex structures were also determined by high-resolution NMR spectroscopy.[12] Briefly, in aqueous buffer containing potassium ions, *Htelo1* was shown to exchange between four distinct G-quadruplex structures, all of which have a mix of parallel and antiparallel strand orientations around a core of three stacked G-tetrads. The CD spectrum of *Htelo1* in aqueous solution exhibits a maximum absorption band near 295 nm and a shoulder at 265 nm (Figure 1). In contrast, when polyethylene glycol (PEG 200) is added to 40% v/v (hereafter referred as to 40% PEG 200), *Htelo1* adopts a parallel-stranded fold. The CD spectrum of *Htelo1* in 40% PEG 200 has a maximum near 265 nm and a minimum near 240 nm (Figure 1). Thus, CD spectroscopy can be used to distinguish between the aqueous solution structures and the parallel-stranded structure of *Htelo1*.

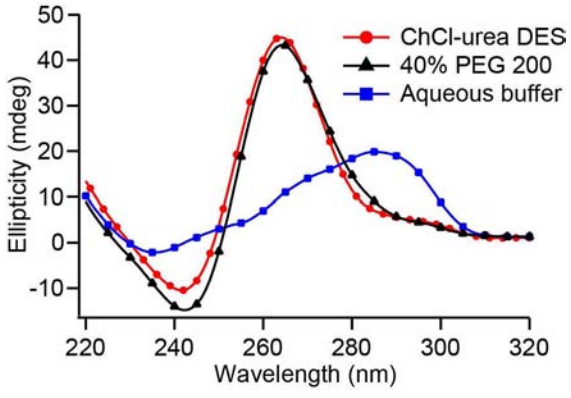

Figure 1. CD spectra of DNA with the HTS-derived sequence d[$TAG_3(TTAG_3)_3$] (*Htelo1*) in various solvents. DES sample was 1 m*m* in nucleotide and contained 100 m*m* KCl. Aqueous buffer solutions contained 20 m*m* potassium phosphate buffer, pH 7. PEG 200 solution was 40% v/v. Spectra were recorded at 20 °C.

The CD spectrum of *Htelo1* in the choline chloride–urea DES, with 100 m*m* KCl added to stabilize G-quadruplex structures,[39] is compared in Figure 1 with the spectra of *Htelo1* in aqueous solution and in 40% PEG 200. The spectrum of *Htelo1* in DES is very close to that observed in 40% PEG 200, establishing that *Htelo1* adopts the same fold in both solvents.

Monitoring of CD spectra during subsequent heating and cooling cycles revealed a single cooperative and reversible transition with a temperature midpoint (T_m) of 77 °C (Figure S1), which is between the T_m of 63 °C observed in an aqueous buffer (Figure S2) and the T_m of 91 °C measured in 40% PEG 200 (Figure S3). Heating and cooling traces of *Htelo1* in the DES exhibited significant hysteresis (>10 °C), indicating that the refolding kinetics of *Htelo1* in the DES is slow on the time scale of sample cooling (ca. 3 h).

The HTS DNA Structure Becomes Kinetically Trapped for Extended Periods When Quick Cooled in the DES. To explore the kinetics of *Htelo1* folding at different temperatures from its thermally denatured state, a series of *Htelo1* samples in the DES were heated to 90 °C, cooled to selected temperatures in less than 2 min, and monitored by CD spectroscopy (Figure 2). These experiments revealed that *Htelo1* in the DES undergoes multiple refolding events when returning to its thermodynamically favored structure. Plots of the 295 nm CD intensity versus time illustrate that *Htelo1* initially folds to a structure, or family of structures, within 1−2 h after being quick cooled to temperatures between 20 and 50 °C (Figure 2B). Least-squares fits of these plots reveal time constants for this transition (τ_1) of 24−16 min for refolding temperatures between 30 and 50 °C, respectively, and around 1 h at 20 °C (Table 1). The rise of the 295 nm CD band intensity is transient with time, illustrating that at least some of the structures adopted by *Htelo1* during the first folding event are only kinetically favored structures.

The CD spectrum of *Htelo1* after the first folding event is different from the equilibrium spectra of *Htelo1* in the DES or in aqueous solution. A time series of spectra collected during *Htelo1* folding at 40 °C is shown in Figure 2A and C. The spectrum of *Htelo1* in this intermediate state has positive bands at 265 and 295 nm, which indicates the presence of one or more G-quadruplex folds that contain both parallel and antiparallel strand orientations.[36] Similar intermediate spectra are observed for samples refolded at 20, 30, 35, and 50 °C (Figure S4). For no temperature investigated between 20 and 50 °C could the intermediate spectra be fit as a linear combination of the equilibrium aqueous and DES spectra of *Htelo1*, indicating that quick cooling traps at least some of *Htelo1* in an alternative state, or in a different distribution of structures as compared to those adopted in aqueous solvent.

The more gradual increase in the 265 nm CD band intensity (Figure 2D) continues at all refolding temperatures until the *Htelo1* sample spectrum eventually returns to that of the parallel G-quadruplex spectrum. The 265 nm CD intensity can therefore be used to follow the transition of *Htelo1* out of the intermediate state. Least squares fits of 265 nm CD intensity versus time (for time >2 × τ_1, Figure 2D) provided rate constants for this second transition as a function of refolding temperature (τ_2, Table 1). In contrast to the first refolding event, this second transition shows substantial temperature dependence. For example, τ_2 = 4.2 h at 50 °C, whereas τ_2 >1600 h at 20 °C. Thus, even though the DES is a liquid at 20 °C, refolding of *Htelo1* to its thermodynamically favored state in the DES can require over 6 months for 95% structure conversion!

dx.doi.org/10.1021/ja303499m | J. Am. Chem. Soc. 2012, 134, 15324−15330

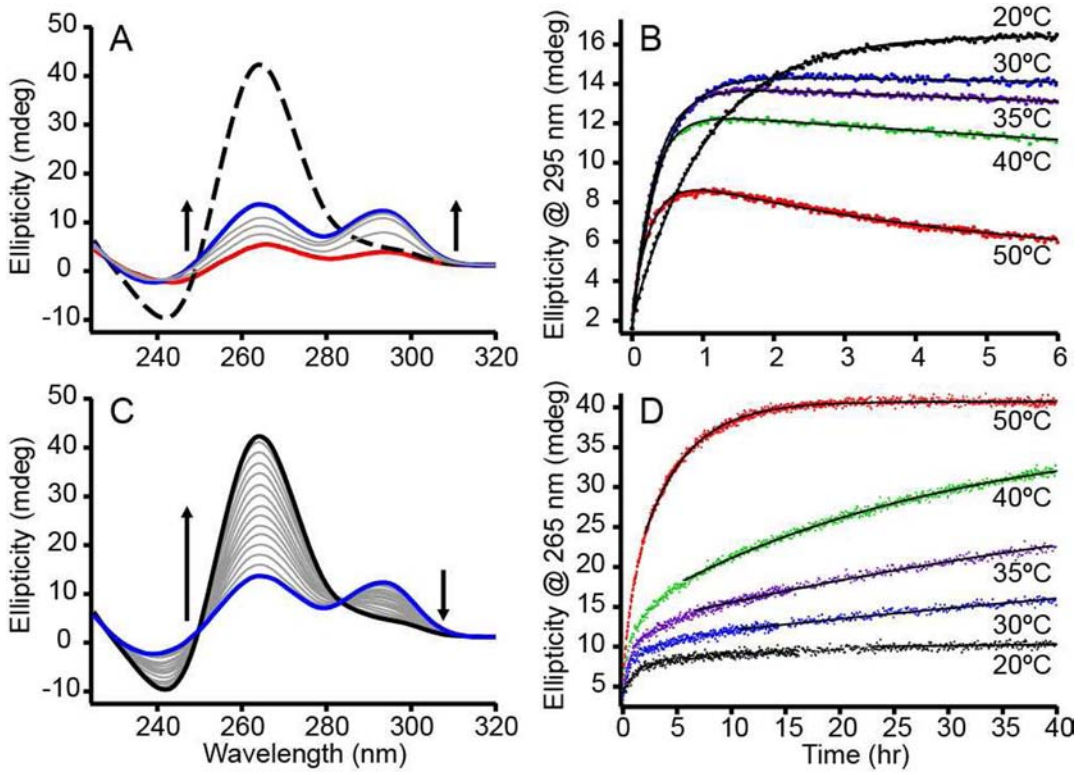

Figure 2. Kinetic analysis of folding *Htelo1* in 100% ChCl/urea DES. (A) Time-dependent CD spectra of quick-cooled *Htelo1* in 100% DES. Initial spectrum before heating is shown as a bold dashed black line. After being heated to 90 °C for 5 min, the sample was cooled (−0.65 °C/s) and placed in spectropolarimeter at 40 °C (red solid line). The *Htelo1* sample reaches a kinetic intermediate (blue solid line) on the order of 1 h. (B) CD signal intensity at 295 nm versus time for *Htelo1* maintained at different temperatures after quick cooling from 90 °C. (C) Time-dependent CD spectra of quick-cooled *Htelo1* during the second transition while being maintained at 40 °C for times between 1 h (blue line) and 200 h (black line). (D) CD signal intensity at 265 nm versus time for *Htelo1* maintained at different temperatures after quick cooling from 90 °C. All samples were 1 m*m* in nucleotide; 100 m*m* KCl. Least squares fits in panels B and D are indicated by solid black lines.

Table 1. Time Constants for *Htelo1* Folding Following Thermal Denaturation in 100% ChCl−Urea DES

temperature (°C)	τ_1 (h)[a]	τ_2 (h)[b]
50	0.27	4.2
40	0.27	28
35	0.32	69
30	0.39	165
20	1.0	>1600

[a]From fitting of 295 nm CD intensity versus time. [b]From fitting of 265 nm CD intensity versus time for time >2 × τ_1.

Solvent Viscosity Slows HTS DNA Refolding in Accord with Kramers Rate Theory. The extremely long time constants observed for *Htelo1* refolding (i.e., τ_2 in Table 1) have not, to the best of our knowledge, been previously observed for intramolecular G-quadruplex folding in aqueous solution. On the other hand, studies of protein folding have shown that structural transitions slow significantly with increasing solvent viscosity.[25−28] Such observations can be explained by Kramers rate theory, which relates changes in the rate of a diffusion-controlled reaction to solvent friction.[33−35] In particular, molecular movements that involve solvent rearrangement will decrease inversely with the friction experienced between the folding molecule and the solvent. Typically, for solvents with viscosities greater than water (i.e., >1 cP), the rates of diffusion controlled reactions are found to vary linearly with viscosity, as the diffusion of a particle in a solvent, according to the Stokes−Einsten equation, scales directly with dynamic viscosity of the solvent.[21,23] The viscosity of the ChCl−urea DES solvent is ca. 1000 cP at 20 °C,[32] sufficiently high to expect solvent friction to decrease the rate of G-quadruplex refolding.

To test the ability for Kramers rate theory to explain the slow kinetics of *Htelo1* refolding in the ChCl−urea DES, it was necessary to compare refolding time constants for the transition of *Htelo1* between the same two structural states, in at least one other solvent with substantially different viscosity. Heddi and Phan measured time constants for the transition of *Htelo1* from its aqueous folded state to its parallel structure in 40% PEG 200 by transferring an aliquot of *Htelo1* from a PEG-free solution to a second aqueous solution containing PEG 200.[12] The same refolding experiment cannot be carried out while maintaining anhydrous ChCl−urea DES, as transferring *Htelo1* from an aqueous solution to the ChCl−urea DES would necessarily introduce water. Water can be removed from the ChCl−urea DES by vacuum, but the time required for water removal would interfere with measuring the kinetics of refolding. Thus, a mixed ChCl−urea−water solvent was sought that still favors the parallel structure and has a viscosity significantly greater than water. For this purpose, it was determined that approximately 85% ChCl−urea DES (w/w with water) is sufficient for the parallel G-quadruplex structure of *Htelo1* to remain as the thermodynamically favored structure (Figure S5).

For isothermal refolding studies, samples were prepared by mixing one part of aqueous stock solution containing *Htelo1* with nine parts ChCl−urea DES (for a final solvent of 90%

dx.doi.org/10.1021/ja303499m | J. Am. Chem. Soc. 2012, 134, 15324−15330

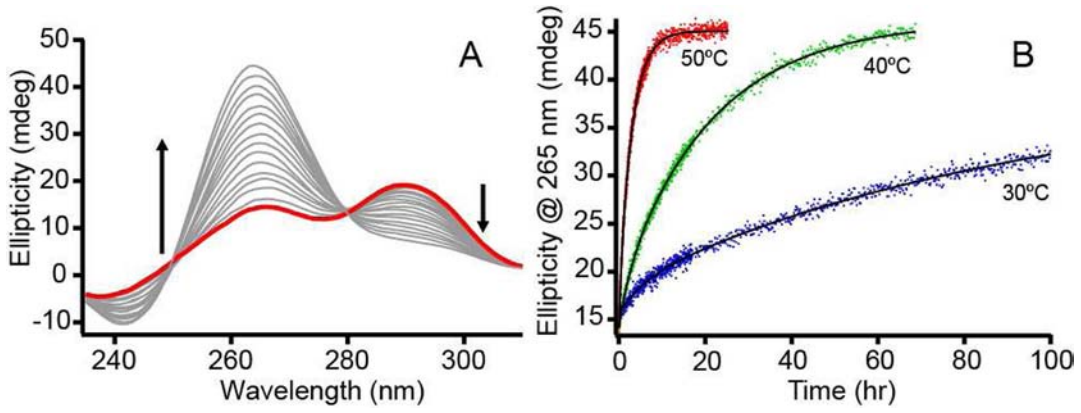

Figure 3. Analysis of *Htelo1* refolding kinetics after transfer from aqueous buffer to 90% ChCl–urea. (A) Time-dependent CD spectra of *Htelo1* following transfer to 90% ChCl–urea. Initial spectrum after transfer is shown in red. (B) CD signal intensity at 265 nm as a function of time. Least-squares fits with double exponential functions are shown as solid lines. All samples were 1 m*m* in nucleotide; 100 m*m* KCl; 20 m*m* potassium phosphate, pH 7.

ChCl–urea DES, 10% water). CD spectroscopy was used to follow the refolding of *Htelo1* in samples maintained at 30, 40, and 50 °C. Example time-course CD spectra for the 40 °C sample are shown in Figure 3A. Isosbestic points at 250 and 280 nm are suggestive of a two-state transition over time, between the aqueous state structures and the parallel structure. To more rigorously test this possibility, we performed a dual wavelength parametric test of the CD data.[40] Inspection of residuals from a linear fit to the plot resulting from this test revealed evidence of deviation from a two-state transition during refolding (Figure S6A). Similar observations resulted from the analysis of data from samples incubated at 30 and 50 °C (Figure S7). In contrast, a similar analysis of data resulting from refolding in 40% PEG 200 did not reveal any evidence of a deviation from a two-state transition (Figures S6B and S8). The implications of these results are discussed below.

Curve fitting of plots of 265 nm CD signal intensity versus time (Figure 3B) revealed principal time constants for conversion between the aqueous folded state and the parallel structure of 94, 22, and 3 h at 30, 40, and 50 °C, respectively (τ_4, Table 2). Fitting each of these curves within one standard deviation of the data required a double exponential function, as a minor fraction of *Htelo1* (estimated to be <10% based on percentage change in CD signal intensity) made the transition to the parallel structure with a time constant that was an order of magnitude less than the major transition (τ_3, Table 2). The significance of observing a separate time constant for a minor fraction of *Htelo1* is also discussed below.

Table 2. Time Constants for *Htelo1* Transition from Aqueous Structures to Parallel Fold in 90% ChCl–Urea DES

temperature (°C)	τ_3 (h)[a]	τ_4 (h)[b]
50	0.43	3.0
40	2.4	22
30	5.6	94

[a]First time constant from fitting of 265 nm CD intensity versus time. [b]Second time constant from fitting of 265 nm CD intensity versus time.

Plotting $\ln(1/\tau_4)$ versus $1/T$ and fitting these data points with the Arrhenius equation yielded an apparent transition barrier height of 139 kJ/mol (Figure 4). For comparison, the rates obtained by Heddi and Phan for the refolding of *Htelo1* in 40% PEG 200 indicate a transition barrier height of 136 kJ/mol.[12] Accordingly, the linear fits of the Arrhenius plots for *Htelo1* refolding in 90% DES and 40% PEG 200 have very similar slopes (Figure 4). However, consistent with the much longer refolding times of *Htelo1* in 90% DES, the Arrhenius plot for this solvent is displaced vertically on the graph in accord with much slower refolding kinetics.

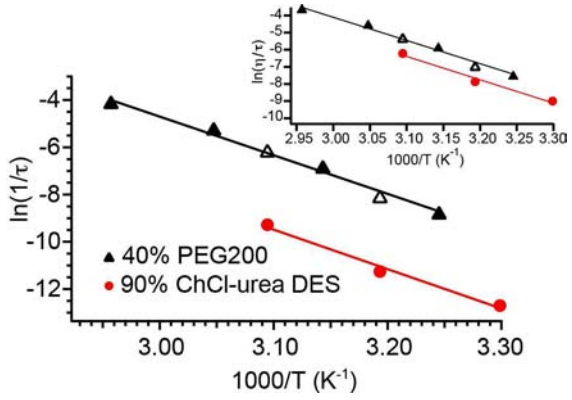

Figure 4. Arrhenius plot comparison for *Htelo1* transition kinetics from aqueous structures to the parallel fold in two solvents. "▲" are data from Heddi and Phan[12] for refolding in 40% PEG 200. Red "●" are from refolding in 90% ChCl–urea DES. Samples contained 1 m*m* DNA, 100 m*m* KCl, 20 m*m* potassium phosphate, pH 7. "△" are data from the current study for *Htelo1* refolding in 40% PEG 200, 100 mM KCl, 20 mM potassium phosphate, pH 7 (Figure S8). (Inset) Arrhenius plot comparison of *Htelo1* DNA transition kinetics in 40% PEG 200 and 90% ChCl–urea DES with rates scaled according to the viscosity of each solvent at each temperature.

The similar slope but vertical placement of the 90% DES and the 40% PEG 200 Arrhenius plots indicate a substantial difference in the pre-exponential constant of the Arrhenius equations that describe these two sets of refolding rates. This vertical displacement represents the approximately 25-fold difference that is observed between refolding rates at corresponding temperatures in the two solvents (Figure 4). As mentioned above, for folding reactions in the strong friction regime, Kramers rate theory and the Stokes–Einstein equation predict that the pre-exponential constant of the Arrhenius equation will decrease linearly with viscosity.[21] That is, the Arrhenius equation can be written as $(1/\tau) = (A/\eta)$

dx.doi.org/10.1021/ja303499m | J. Am. Chem. Soc. 2012, 134, 15324–15330

$\exp^{(-\Delta G/RT)}$, where η is solvent viscosity and A is the component of the preexponential constant that does not vary with solvent viscosity. To examine the consistency of this form of the Arrhenius equation with *Htelo1* refolding, the natural log of refolding rates were replotted versus $1/T$ as viscosity-adjusted rates (i.e., $\ln(\eta/\tau)$ versus $1/T$) (Figure 4, inset). Viscosities used for this adjustment are provided in Table S1. A linear fit of these viscosity-adjusted rates yields a slope of 113 kJ/mol for both solvents. The closer vertical placement of the two plots, now within a factor of 2.5, is in accordance with the prediction of Kramers rate theory. Specifically, at least a factor of 10 of the 25-fold difference in *Htelo1* refolding rates for the two solvents can be attributed to solvent viscosity. Additionally, the 20% decrease in the apparent activation barrier in both solvents illustrates the influence of temperature-dependent solvent viscosity on the apparent enthalpy of the transition state barrier height. Possible reasons for a greater than linear slowing of refolding rates with increased bulk viscosity are discussed below.

Evidence for a Solvent-Selected G-Quadruplex Folding Pathway. A potential means to compare *Htelo1* folding in the water-free (i.e., 100%) ChCl−urea DES with folding in the 40% PEG 200 solution is to evaluate the rates for folding of thermally denatured *Htelo1* in both solvents. As shown above, the folding of *Htelo1* after quick cooling resulted in the trapping of *Htelo1* in an intermediate state for hours to months, before eventual conversion back to the parallel-stranded fold. An attempt was made to also measure the rate of *Htelo1* folding in 40% PEG 200 after quick cooling from its thermally denatured state. However, in contrast to the pathway observed in 100% ChCl−urea DES, it was found that *Htelo1* in 40% PEG 200 returned to its parallel fold in less than 2 min at 20 °C (Figure S9). Although the time resolution of these CD-monitored experiments did not allow a quantitative comparison of folding rates between *Htelo1* in 100% DES and 40% PEG 200, a qualitative comparison is still of interest. In particular, we emphasize that the parallel-stranded G-quadruplex of *Htelo1* is the thermodynamically favored structure in both solvents. Nevertheless, in 100% ChCl−urea DES, a significant fraction of *Htelo1* folds into an alternative, kinetically favored structure, at temperatures ranging between 20 and 50 °C. Complete transition from this intermediate state to the parallel structure required several months at room temperature. If *Htelo1* folded to the same intermediate state when quick cooled in the 40% PEG 200 solution, the rate increase for exiting this intermediate state would be on the order of 5×10^4 (i.e., $\tau_2/\tau_{PEG} > 1600$ h/2 min). Because the viscosities of the two solvents at room temperature only differ by a factor of approximately 200 (far less than 5×10^4), a more reasonable explanation for the much greater difference in time required to reach the parallel fold is that the folding pathway of *Htelo1* is solvent dependent. That is, folding in the 100% DES directs *Htelo1* to an intermediate state that is not accessed during folding in 40% PEG 200.

DISCUSSION

We have shown that *Htelo1*, DNA with a nucleotide sequence derived from the human telomere sequence (HTS), adopts the parallel G-quadruplex fold in an anhydrous ChCl−urea DES. Previous studies had shown that cosolvents in aqueous solutions (e.g., acetonitrile and polyethylene glycol) can shift the equilibrium structure of HTS DNA from the mixed parallel, antiparallel G-quadruplex folds that are favored in aqueous solutions to the parallel fold that was first observed in the crystal state.[12,14] Our observation that *Htelo1* adopts its parallel fold in solutions that contain 85−100% ChCl−urea (0−15% water) supports previous conclusions that dehydration (or osmotic stress), rather than molecular crowding, drives HTS DNA to parallel G-quadruplex structures.[14] However, as a cosolvent with water, the ChCl−urea mixture is qualitatively less effective than PEG 200 in shifting *Htelo1* to the parallel fold, as the parallel fold of *Htelo1* is favored in a 40% PEG 200 solution that contains 60% water. Similarly, 40% acetonitrile is able to significantly shift the structural equilibrium of a related DNA sequence to the parallel form,[14] whereas a water−DES mixture with 40% ChCl−urea shows minimal change (ca. 10% or less) from the aqueous folded state (Figure S5). This requirement for less water in a mixed solvent with ChCl−urea may be the result of choline and urea being able to occupy some solvent-accessible sites on *Htelo1* in a manner similar to that of water, as the alcohol group of choline and the amino and carbonyl groups of urea could replace water molecules that are H-bound donors or acceptors. In contrast, the larger size of PEG 200 could restrict substitution of water-occupied sites on the surface of a G-quadruplex. The molecular-level solvent properties of acetonitrile are also expected to be more different from water than those of choline and urea.

Previous studies have shown that folding of an intramolecular HTS G-quadruplex at 25 °C, after the addition of cations necessary for G-tetrad formation, takes place within 20 ms[41] to 1.5 min,[42] with evidence of intermediate (i.e., kinetically favored) folds being assumed over the course of folding. In the 100% ChCl−urea DES, folding of *Htelo1* after quick cooling from its thermally denatured state is considerably slower (around 1 h), with intermediate folded states being adopted for extended periods (up to several months). As mentioned above, decreased diffusion rates, which are inversely related to solvent viscosity through the Stokes−Einstein equation, can slow folding transition times as predicted by Kramers rate theory.[21] The tremendous temperature dependence observed for *Htelo1* conversion between its kinetically favored state and the parallel fold in 100% DES (e.g., τ_2 >1600 h at 20 °C; τ_2 = 4.2 h at 50 °C) could therefore be due to both a relatively large enthalpy barrier (i.e., >100 kJ/mol) and a decrease in the rate of DNA chain diffusion as a result of the DES viscosity decreasing by about a factor of 10 from 20 to 50 °C (i.e., from ca. 1100 to ca. 100 cP, respectively). In contrast, we observe that the first folding transition of *Htelo1* after quick cooling (i.e., τ_1) has only a modest dependence on temperature and solvent friction. For example, there is only a factor of 1.2 increase in the time constant for intermediate structure formation at 35 °C as compared to 50 °C (0.32 and 0.27 h, respectively), whereas the 100% DES viscosity decreases about a factor of 3 for the same temperature range (from ca. 300 to ca. 100 cP, respectively).[32] The lack of an inverse relationship between folding rates and solvent viscosity indicates that the initial folding pathway of *Htelo1* after quick cooling does not have a diffusion-limited component that requires appreciable solvent rearrangement.[21] However, the minimal temperature dependence of this transition does indicate that the primary contribution to the free energy barrier of refolding is entropic in nature. Thus, the primary entropic term for initial folding is apparently associated with internal rearrangements, as has been observed for some transitions associated with protein folding.[43]

The dramatically different time scales required for *Htelo1* to reach its thermodynamically favored structure after thermal denaturation in the 100% DES as compared to analogous

folding in 40% PEG 200 (i.e., up to 5×10^4 times slower) also illustrate the ability for nonaqueous/viscous solvents to direct the folding of macromolecules to alternative structures that are not necessarily kinetically favored or accessible in aqueous solvent. Even though *Htelo1* quick cooled to 20 °C in the 100% DES eventually folds to the thermodynamically-favored parallel structure, it exists in an alternative folded state for months at room temperature. For most laboratory experiments, such times scales are equivalent to "permanent" trapping in an alternative (solvent-directed) structure. Viscosity-altered kinetics during protein folding has been shown to influence the adoption of alternative structures,[21,44,45] and the present study shows that this phenomenon could be even more dramatic for nucleic acids.

Our comparison of the time constants associated with the *Htelo1* structural transition from its mixed antiparallel, parallel folded state in aqueous solution to its parallel fold in 90% ChCl–urea DES with time constants for the same transition in 40% PEG 200 provide solid evidence that G-quadruplex folding can be altered by solvent viscosity in accordance with Kramers rate theory. Most studies of protein folding kinetics as a function of solvent viscosity have shown less than an inverse dependence of folding rate with solvent viscosity. That is, $1/\tau \propto 1/\eta^n$, with $n < 1$. Typically, the exponent of viscosity approaches unity with increasing viscosity.[23] In the present study, we observe a greater than expected increase in refolding time. Specifically, we observed a 25-fold greater refolding time constant (i.e., τ_4) for 90% ChCl–urea DES as compared to refolding in 40% PEG 200, but the bulk viscosities of these two solvents differ only by a factor of 10. One possibility for this greater than expected increase in refolding time is an overestimation of the solvent viscosity that is experienced by the G-quadruplex in its immediate (microscopic) vicinity. Another possibility is that the solvent friction experienced by *Htelo1* increases more than linearly with the macroscopic dynamic viscosity of 90% ChCl–urea. In this case, the actual solvent friction could be greater than predicted by solvent viscosity if solvent molecules (e.g., choline) associate with the nucleic acid more strongly than water and thereby increase the effective size of nucleic acid structures (e.g., loops) that require solvent rearrangement during refolding.

The refolding of *Htelo1* in 90% DES also illustrated the potential for high viscosity solvents to provide additional information about the initial state of molecules undergoing structural transitions and their differential rates of conversion. As noted above, the parametric plot analysis of *Htelo1* conversion in 90% DES displayed a small, but measurable, deviation from a two-state transition (Figure S6A). This observation is consistent with the curve fitting of CD signal intensity at 265 nm versus time (Figure 3) requiring the use of a double exponential. The time constant associated with this minor fraction of the *Htelo1* sample (i.e., τ_3) is an order of magnitude smaller than the time constant of the main transition (i.e., τ_4). Our observation of multiple rates during refolding is confirmatory of the conclusion of Heddi and Phan that *Htelo1* exists in more than one folded state in the aqueous solution.[12] Moreover, our kinetic measurements provide additional information. Specifically, the free energy barrier of transition to the parallel fold is substantially less for at least one minor species in the aqueous solution, as compared to the other folded species in the same sample. In contrast, different rates of conversion are not observed in similar experiments with the less viscous 40% PEG 200 solvent, as the CD signal intensity at 265 nm versus time is fit well by a single exponential function (Figure S8). Moreover, the two-state transition in the 40% PEG 200 solvent successfully holds up to examination by a parametric plot analysis (Figure S6B). A possible explanation for these solvent-specific differences is that the interaction of *Htelo1* with PEG 200 allows for all aqueous forms of the G-quadruplex to convert with the same transition rates. However, another possible explanation is that the increased viscosity of the 90% ChCl–urea solvent (and associated slower refolding times) allows the different rates of *Htelo1* refolding to be observed.

There are a number of protein folding studies in which Kramers rate theory has been used successfully to explain decreased folding rates with increased solvent viscosity, for folding times ranging from 100 ns to 1s.[21] Likewise, analysis of DNA hairpin folding rates, which takes place on the microsecond time scale, were found to follow an approximately η^{-1} relationship with viscosity.[29,30] In the present study, the structural transitions measured in 90% DES follow the refolding of a nucleic acid from one highly structured state to another. Despite differences in the details of the present study and past studies of protein or nucleic acid folding/refolding, the present study demonstrates that Kramers rate theory is valid for describing the effect of solvent friction on macromolecular folding over another 5 orders of magnitude, that is, up from 1 s in the case of Protein L folding[26] to at least 3.4×10^5 s (94 h) for *Htelo1* refolding. Overall, it appears that Kramers rate theory has now been shown to be applicable for describing solvent effects on macromolecular folding kinetics over more than 12 orders of magnitude (i.e., 100 ns to $>10^5$ s).

■ CONCLUSIONS

We have demonstrated that the human telomere sequence in anhydrous ChCl–urea DES adopts a parallel-stranded G-quadruplex, specifically the "propeller" type topology observed in solution with 40% PEG 200 and first observed in the crystal state. Folding of *Htelo1* in the anhydrous ChCl–urea DES and mixed DES–water solvents has revealed diffusion-limited kinetics consistent with Kramers rate theory. To the best of our knowledge, this is the first investigation of G-quadruplex kinetic properties as a function of viscosity. We have shown that by utilizing a high viscosity solvent, and thereby changing diffusion rates, HTS G-quadruplex refolding along the free energy landscape can be explored in greater detail. Moreover, future investigations of G-quadruplexes should take into account solvent friction effects, as in vivo folding is likely to be affected by solvent viscosity, given that the viscosity of the cellular milieu is as high as 140 cP.[46] Finally, we expect that many other nucleic acid structures, particularly globular RNAs, will be found to show similar behavior in high viscosity solvents, and that viscosity could be harnessed for use in DNA nanotechnology where time-dependent structures are desired.[47]

■ METHODS

Sample Preparation. DNA oligonucleotides were purchased from Integrated DNA Technologies (Coralville, IA). The concentrations of DNA stock solutions were determined on the basis of UV absorption. The choline chloride/urea DES was prepared by heating a 1:2 molar mixture of choline chloride (Acros Organics) and urea (Fisher) anhydrous solids while stirring at 80 °C until a liquid was formed (ca. 2 h). Water content of the DES, measured using the Hydranal moisture test kit based on Karl Fischer analysis (Sigma-Aldrich), was established to be <0.25%.[31] Solutions of nucleic acids in the 100% DES

solvent were prepared by mixing aqueous stock solutions of DNA and KCl with the DES, and then subjecting the mixture to vacuum centrifugation until a constant mass was reached (at least 12 h), which indicated the quantitative removal of water from the anhydrous DES within the experimental error of gravimetric analysis (~0.1% of sample weight). Prior to analysis the G-quadruplex DNA was equilibrated by heating the samples in the relevant solvent for 5 min at 90 °C and then slowly annealing over the course of 12 h (−6 °C/h) to room temperature.

CD Spectrophotometry. CD spectra were acquired on a Jasco J-810 spectropolarimeter with a Peltier temperature controller and 1 mm path length cells. Unless otherwise stated, spectra were acquired by scanning 220−320 nm at a rate of 500 nm/min, with averaging of three measurements. For thermal denaturation studies, measurements were taken over heating/cooling cycles from 5−95 °C (DES), 5−90 °C (H_2O), and 50−106 °C (40% PEG 200) at increments of 2 °C (100% DES and 40% PEG 200) or 5 °C (H_2O). For kinetic studies, samples were scanned at a rate of 1000 nm/min, with averaging of two measurements.

Viscosity Measurements. Dynamic viscosity of the 90% DES solution was determined using a RheSys Merlin II rotational viscometer with an integrated temperature controller and cup and bob attachment. The apparatus was calibrated using two viscosity standards (Brookfield, VWR). The instrument error of the 96 cP standard was −0.86%, and it was +26% for the 9.2 cP standard. Sample solutions of the 90% DES were prepared using airtight bottles and contained 90% DES by mass, 100 m*m* KCl, and 20 m*m* KPO_4, pH 7. Viscosity measurements were replicated thrice for each sample. Values reported are average values with linearly interpolated error percent.

■ ASSOCIATED CONTENT

Ⓢ Supporting Information

Supplementary tables and figures. This material is available free of charge via the Internet at http://pubs.acs.org.

■ AUTHOR INFORMATION

Corresponding Author

hud@chemistry.gatech.edu

Notes

The authors declare no competing financial interest.

■ ACKNOWLEDGMENTS

This work was jointly supported by the NSF and the NASA Astrobiology Program, under the NSF Center for Chemical Evolution, CHE-1004570. We thank Professors L. D. Willams, C. Liotta, C. Eckert, and E. Biddinger for helpful discussions.

■ REFERENCES

(1) McEachern, M. J.; Krauskopf, A.; Blackburn, E. H. *Annu. Rev. Genet.* **2000**, *34*, 331−358.
(2) de Lange, T. *Science* **2009**, *326*, 948−952.
(3) Moyzis, R. K.; Buckingham, J. M.; Cram, L. S.; Dani, M.; Deaven, L. L.; Jones, M. D.; Meyne, J.; Ratliff, R. L.; Wu, J. R. *Proc. Natl. Acad. Sci. U.S.A.* **1988**, *85*, 6622−6626.
(4) Meyne, J.; Ratliff, R. L.; Moyzis, R. K. *Proc. Natl. Acad. Sci. U.S.A.* **1989**, *86*, 7049−7053.
(5) *Quadruplex Nucleic Acids*; Neidle, S., Balasubramanian, S., Eds.; RSC Publishing: Cambridge, 2006.
(6) Neidle, S. *FEBS J.* **2010**, *277*, 1118−1125.
(7) Mergny, J. L.; Helene, C. *Nat. Med.* **1998**, *4*, 1366−1367.
(8) Phan, A. T. *FEBS J.* **2010**, *277*, 1107−1117.
(9) Webba da Silva, M. *Chem.-Eur. J.* **2007**, *13*, 9738 −9745.
(10) Lane, A. N.; Chaires, J. B.; Gray, R. D.; Trent, J. O. *Nucleic Acids Res.* **2008**, *36*, 5482−5515.
(11) Li, J.; Correia, J. J.; Wang, L.; Trent, J. O.; Chaires, J. B. *Nucleic Acids Res.* **2005**, *33*, 4649−4659.
(12) Heddi, B.; Phan, A. T. n. *J. Am. Chem. Soc.* **2011**, *133*, 9824−9833.
(13) Xue, Y.; Kan, Z. Y.; Wang, Q.; Yao, Y.; Liu, J.; Hao, Y. H.; Tan, Z. *J. Am. Chem. Soc.* **2007**, *129*, 11185−11191.
(14) Miller, M. C.; Buscaglia, R.; Chaires, J. B.; Lane, A. N.; Trent, J. O. *J. Am. Chem. Soc.* **2010**, *132*, 17105−17107.
(15) Miyoshi, D.; Karimata, H.; Sugimoto, N. *J. Am. Chem. Soc.* **2006**, *128*, 7957−7963.
(16) Vorlíčková, M.; Bednářová, K.; Kejnovská, I.; Kypr, J. *Biopolymers* **2007**, *86*, 1−10.
(17) Oganesian, L.; Bryan, T. M. *BioEssays* **2007**, *29*, 155−165.
(18) Hänsel, R.; Löhr, F.; Foldynová-Trantírková, S.; Bamberg, E.; Trantírek, L.; Dötsch, V. *Nucleic Acids Res.* **2011**, *39*, 5768−5775.
(19) Renciuk, D.; Kejnovska, I.; Skolakova, P.; Bednarova, K.; Motlova, J.; Vorlickova, M. *Nucleic Acids Res.* **2009**, *37*, 6625−6634.
(20) Lee, J. Y.; Okumus, B.; Kim, D. S.; Ha, T. *Proc. Natl. Acad. Sci. U.S.A.* **2005**, *102*, 18938−18943.
(21) Hagen, S. J. *Curr. Protein Pept. Sci.* **2010**, *11*, 385−395.
(22) Jas, G. S.; Eaton, W. A.; Hofrichter, J. *J. Phys. Chem. B* **2000**, *105*, 261−272.
(23) Ansari, A.; Jones, C. M.; Henry, E. R.; Hofrichter, J.; Eaton, W. A. *Science* **1992**, *256*, 1796−1798.
(24) Best, R. B.; Hummer, G. *Phys. Rev. Lett.* **2006**, *96*, 228104.
(25) Jacob, M.; Geeves, M.; Holtermann, G.; Schmid, F. X. *Nat. Struct. Biol.* **1999**, *6*, 923−926.
(26) Plaxco, K. W.; Baker, D. *Proc. Natl. Acad. Sci. U.S.A.* **1998**, *95*, 13591−13596.
(27) Ramos, C. H.; Weisbuch, S.; Jamin, M. *Biochemistry* **2007**, *46*, 4379−4389.
(28) Perl, D.; Jacob, M.; Bánó, M.; Stupák, M.; Antalik, M.; Schmid, F. X. *Biophys. Chem.* **2002**, *96*, 173−190.
(29) Ansari, A.; Kuznetsov, S. V. *J. Phys. Chem. B* **2005**, *109*, 12982−12989.
(30) Wallace, M. I.; Ying, L.; Balasubramanian, S.; Klenerman, D. *Proc. Natl. Acad. Sci. U.S.A.* **2001**, *98*, 5584−5589.
(31) Mamajanov, I.; Engelhart, A.; Bean, H.; Hud, N. *Angew. Chem., Int. Ed.* **2010**, *49*, 6310−6314.
(32) Abbott, A. P.; Capper, G.; Davies, D. L.; Rasheed, R. K.; Tambyrajah, V. *Chem. Commun.* **2003**, 70−71.
(33) Kramers, H. A. *Physica* **1940**, *7*, 284−304.
(34) Hanggi, P.; Talkner, P.; Borkovec, M. *Rev. Mod. Phys.* **1990**, *62*, 251−341.
(35) Hynes, J. T. *Annu. Rev. Phys. Chem.* **1985**, *36*, 573−597.
(36) Karsisiotis, A. I.; Hessari, N. M. a.; Novellino, E.; Spada, G. P.; Randazzo, A.; Webba da Silva, M. *Angew. Chem., Int. Ed.* **2011**, *50*, 10645−10648.
(37) Masiero, S.; Trotta, R.; Pieraccini, S.; De Tito, S.; Perone, R.; Randazzo, A.; Spada, G. P. *Org. Biomol. Chem.* **2010**, *8*, 2683−2692.
(38) Paramasivan, S.; Rujan, I.; Bolton, P. H. *Methods* **2007**, *43*, 324−331.
(39) Engelhart, A. E.; Plavec, J.; Persil, O.; Hud, N. V. In *Nucleic Acid-Metal Ion Interactions*; Hud, N. V., Ed.; RCS Publishing: Cambridge, 2009; pp 118−153.
(40) Wallimann, P.; Kennedy, R. J.; Miller, J. S.; Shalongo, W.; Kemp, D. S. *J. Am. Chem. Soc.* **2003**, *125*, 1203−1220.
(41) Gray, R. D.; Chaires, J. B. *Nucleic Acids Res.* **2008**, *36*, 4191−4203.
(42) Zhao, Y.; Kan, Z. Y.; Zeng, Z. X.; Hao, Y. H.; Chen, H.; Tan, Z. *J. Am. Chem. Soc.* **2004**, *126*, 13255−13264.
(43) Pabit, S. A.; Roder, H.; Hagen, S. J. *Biochemistry* **2004**, *43*, 12532−12538.
(44) Rhee, Y. M.; Pande, V. S. *J. Phys. Chem. B* **2008**, *112*, 6221−6227.
(45) Narayanan, R.; Pelakh, L.; Hagen, S. J. *J. Mol. Biol.* **2009**, *390*, 538−546.
(46) Kuimova, M. K.; Yahioglu, G.; Levitt, J. A.; Suhling, K. *J. Am. Chem. Soc.* **2008**, *130*, 6672−6673.
(47) Krishnan, Y.; Simmel, F. C. *Angew. Chem., Int. Ed.* **2011**, *50*, 3124−3156.